Journal of Nuclear Materials 407 (2010) 205–210

Contents lists available at ScienceDirect

Journal of Nuclear Materials

journal homepage: www.elsevier.com/locate/jnucmat

A study of early corrosion behaviors of FeCrAl alloys in liquid lead–bismuth eutectic environments

Jun Lim [a,b], Hyo On Nam [a], Il Soon Hwang [a], Ji Hyun Kim [b,*]

[a] Nuclear Transmutation Energy Research Center of Korea (NUTRECK), Seoul National University, San 56-1 Shinlim-dong, Gwanak-ku, Seoul 151-742, Republic of Korea
[b] Interdisciplinary School of Green Energy, Ulsan National Institute of Science and Technology, 100 Banyeon-ri, Eonyang-eup, Ulju-gun, Ulsan 689-798, Republic of Korea

ARTICLE INFO

Article history:
Received 9 March 2009
Accepted 20 October 2010

ABSTRACT

Lead and lead–bismuth eutectic (LBE) alloy have been increasingly receiving attention as heavy liquid metal coolants (HLMC) for future nuclear energy systems. The compatibility of structural materials and components with lead–bismuth eutectic liquid at high temperature is one of key issues for the commercialization of lead fast reactors. In the present study, the corrosion behaviors of iron-based alumina-forming alloys (Kanthal-AF®, PM2000, MA956) were investigated by exposing to stagnant LBE environments at 500 °C and 550 °C for up to 500 h. After exposures, the thickness and chemistry of the oxide layer on the specimens were analyzed by scanning electron microscopy, scanning transmission electron microscopy and energy dispersive X-ray spectroscopy. As a result, the oxide characteristics and the corrosion resistance were compared. In this study, it was shown that the corrosion resistance of FeCrAl ODS steels (PM2000, MA956) are superior to that of FeCrAl ferritic steel (Kanthal-AF®) in higher temperature LBE.

1. Introduction

Lead–bismuth eutectic (LBE) alloy is one of coolant candidates in the generation fourth (Gen-IV) and small- and medium-sized reactor (SMR) nuclear systems because of its low melting temperature, high boiling point, excellent chemical stability, no fire or explosion and neutron transparency. In addition, LBE has high capability for natural circulation [1]. In recent years, lead and LBE have attracted intensifying attention and increasing R&D efforts in worldwide, due to global interests firstly in partition and transmutation, and secondly in nuclear systems utilizing fast neutron [2,3]. In the same respect, the Nuclear Transmutation Energy Research Center of Korea (NUTRECK) of Seoul National University in the Republic of Korea is developing an innovative technology to burn spent nuclear fuels into low-intermediate level waste by utilizing the LBE cooled PEACER [4] and its small modular reactor design, PASCAR [5].

Those LBE-cooled nuclear energy systems, however, have been exposed to several issues arising from the limitation of system life due to their relatively low corrosion resistance of structural materials in the LBE environments. The corrosion behaviors on several types of austenitic and ferritic/martensitic (FM) steels have been extensively studied to investigate the corrosion performance of structural materials and improve the materials life performance worldwide [6]. While it was confirmed that both FM steels and austenitic steels maintain protective oxide layer at temperature below 500 °C with an adequate oxygen concentration in LBE, the oxide layer becomes non-protective at temperature above 500 °C. Both materials, therefore, are generally restricted to use at temperatures below 500 °C in LBE.

For long term and high temperature (>500 °C) application, Al-containing alloy and Al-coated steels have been recently investigated [7–11]. Coating surfaces of FeCr steels with FeCrAlY after homogenization by melting with the GESA pulse has shown an excellent corrosion protection at up to 650 °C in LBE [7–9]. Impervious thin alumina scales were formed to protect steels from dissolution attack by LBE as well as from internal oxidation.

In the present study, the early corrosion behaviors of three types of iron-based alumina-forming alloys were investigated to understand fundamental procedures of corrosion by exposure to stagnant LBE followed by nano-structural examination of surface film and adjacent metal.

2. Experimental

Three iron-based alumina-forming alloys were selected in this study with their chemical composition given in Table 1. One is Kanthal-AF® which was manufactured by Sandvik and an FeCrAl alloy containing small amount of yttrium and zirconium. The other two alloys are MA956 and PM2000 which are both yttrium-oxide dispersion strengthened (ODS) steels. The ODS steels were supplied by Special Metals Corp. and Plansee GmbH, respectively.

All specimens were machined to plates with the dimension of 15 mm in length, 8 mm in width and 1 mm in thickness. Before

* Corresponding author. Tel.: +82 52 217 2913.
E-mail address: kimjh@unist.ac.kr (J.H. Kim).

0022-3115/$ - see front matter © 2010 Elsevier B.V. All rights reserved.
doi:10.1016/j.jnucmat.2010.10.018

Table 1
Chemical composition of the tested materials, wt.%.

Materials	Fe	Cr	Al	Ti	Y_2O_3	Y	Zr	C	S	Manufacturer
Kanthal-AF®	Bal.	22.3	5.1			0.05	0.07	0.021	0.004	Sandvik
MA956	Bal.	18.0	4.8	0.4	0.5			0.018	0.008	Special metals
PM2000	Bal.	19.2	5.7	0.5	0.5			0.013	0.007	PLANSEE

the exposure in LBE, each specimen was mechanically polished by abrasive SiC papers down to 600 grits with water cooling and then ultrasonically cleaned with acetone and ethanol, respectively, before the final drying.

The corrosion tests were carried out at 500 and 550 °C for 500 h in static LBE cells that is connected with oxygen control system as described in Fig. 1. An alumina crucible was used as the LBE container in each oxygen-controlled cell. The quantity of LBE in the alumina crucible was nominally 9 kg in weight. During the test, oxygen concentration in LBE was controlled over the range of 10^{-6}–10^{-5} wt.% by flowing H_2/H_2O gas with regulated composition and flow rates, and monitored by yttria-stabilized zirconia (YSZ) oxygen probe that was hermetically sealed using the electromagnetically swaged metal–ceramic joining method for long-term applications [12]. Oxygen-saturated bismuth (Bi/Bi_2O_3) was used as a reference reaction couple that is placed inside YSZ.

After the experiment, the surface layers of each test specimen were examined using field emission-scanning electron microscopy (FE-SEM) and scanning transmission electron microscopy (STEM) couples with energy dispersive X-ray spectroscopy (EDS). Before the nano-structural analysis, the tested specimens were washed in a hot glycerin bath at about 170 °C to remove residual LBE. To analyze the cross section of surface oxide layers on the specimen, the specimens were ion-milled by focused ion beam (FIB) and TEM specimens were also machined by FIB.

3. Results

3.1. Kanthal-AF®

After exposure of Kanthal-AF® to 500 °C stagnant LBE for 500 h, relatively thin (100–200 nm thick) continuous Al_2O_3 layers were observed on the surface of the specimen. As shown in Fig. 2a, no corrosion damage was found by LBE at 500 °C. At 550 °C, however, the corrosion behavior is found to change in the respect of oxide thickness and continuity of oxide layer (Fig. 2b).

The results of STEM/EDS analysis for the specimens tested at 500 °C indicate the existence of the chromium sulfide (CrS) island at the Al_2O_3 layer/metal interface as shown in Fig. 3. These Cr and S co-segregations in the interface are often observed for FeCrAl alloys [13–15]. Voids which may weaken interfacial bonding of oxide [13] were formed at the oxide/sulfide interface as shown in Fig. 2a. It is well known that small amount of reactive element such as Y, Ce, Hf and Zr added in FeCrAl alloys can prevent S segregation to the Al_2O_3/metal interface [13]. In this work, however, S segregated to the oxide/metal interface although Kanthal-AF® contains reactive elements about 500 ppm Y and 700 ppm Zr. As seen from Figs. 2b and 4, the thickness of Al_2O_3 layers was measured to be about 2 μm and LBE was observed to penetrate into the metal through the damaged oxide layer and grain boundary of the metal. The penetration depth of LBE in the metal was about 20 μm.

3.2. MA956

MA956 in this study was observed to show no severe dissolution damage in both 500 °C and 550 °C tests, as shown in Fig. 5. From the results of STEM/EDS analysis in Fig. 6, the corrosion scales were found to consist of three different layers; the outer scale containing Al_2O_3 layer, the middle CrS island, and the inner Al_2O_3 layer. The total corrosion scale formed at 500 °C for 500 h is thicker than that of Kanthal-AF® at the same condition. The scale formed at 550 °C contains more voids at the oxide/CrS interface in comparison with that grown at 500 °C. The inner Al_2O_3 layer formed on MA956 appeared as a protective layer to prevent internal dissolution of metal by LBE.

3.3. PM2000

After exposure of PM2000 to 500 °C and 550 °C in stagnant LBE, respectively, for 500 h, a thin continuous Al_2O_3 layer was formed on the surface and the chromium sulfide (CrS) island at the interface of Al_2O_3 layer and metal as shown in Figs. 7a and 8. The general characteristics of formed oxide scale at 500 °C in this alloy are very similar to that of Kanthal-AF® at the same condition as described in the previous section.

At 550 °C, a lot of voids were observed at the scale/metal interfaces as seen in Kanthal-AF®, but there were scale-spalled region in the oxide layer of PM2000. The detail analysis was performed in the scale-spalled region in this alloy. Fig. 9 shows the FE-SEM image of the cross section in the scale-spalled area of the PM2000

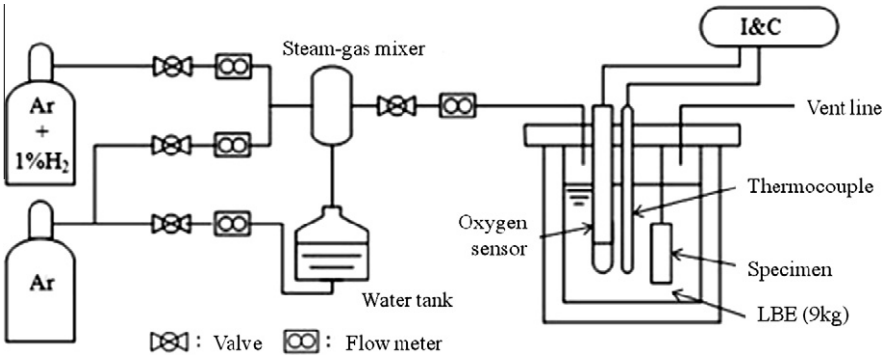

Fig. 1. Schematics of stagnant corrosion test apparatus equipped with oxygen control system.

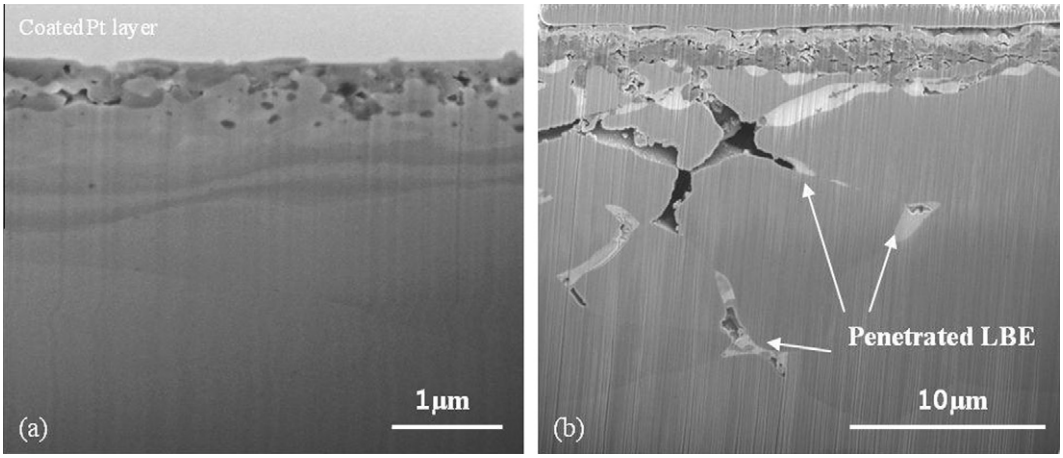

Fig. 2. FE-SEM images of the cross section of Kanthal-AF® after immersion in 500 °C (a) and 550 °C (b) stagnant LBE for 500 h.

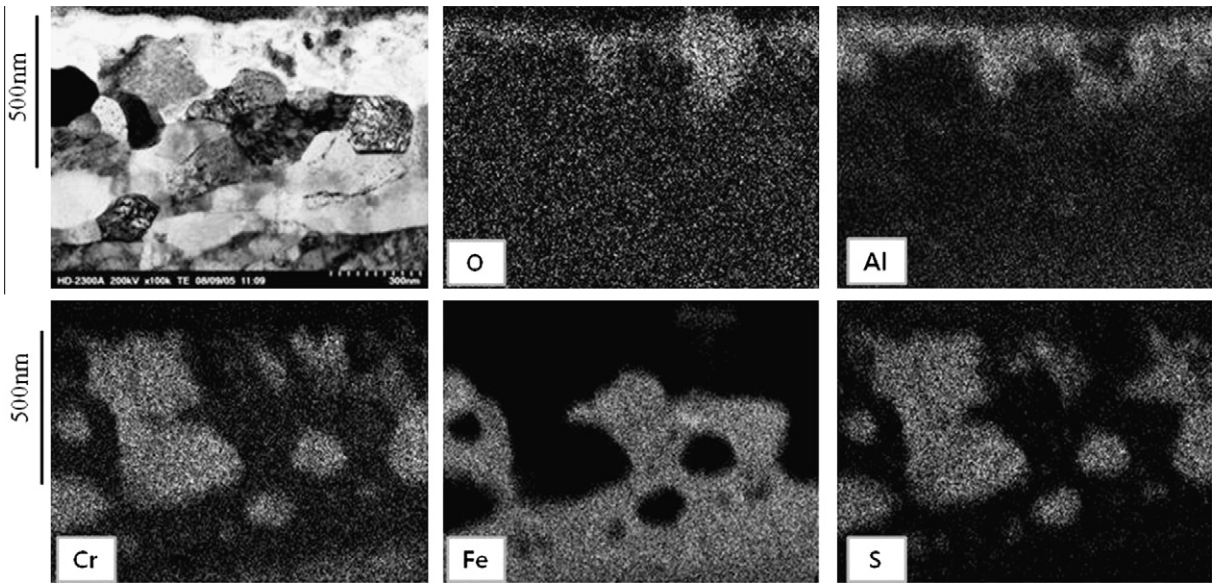

Fig. 3. STEM image and maps of cross sectional chemical composition of Kanthal-AF® after immersion in 500 °C stagnant LBE for 500 h obtained by EDS.

samples after exposure to 550 °C stagnant LBE for 500 h. As shown in Fig. 9, these spalled areas were found to contain LBE inclusion, but there was no LBE penetration into the metal.

4. Discussion

Because the solubility of Al in LBE is higher than that of Cr and Fe, the protectiveness and stability of thermally grown oxide appear to be very important for FeCrAl alloy. Al containing ODS materials (MA956, PM2000) shows good corrosion resistance to LBE up to 550 °C, whereas FeCrAl alloy, Kanthal-AF® did not show good resistance to the dissolution attack by LBE at 550 °C in this study. Although the test materials showed some degree of difference in corrosion behaviors, it was found that there was common behavior of segregation of S and Cr at the oxide/metal interface. The chromium sulfide can act as an obstacle to the diffusion of Al that can heal the defects of outer Al_2O_3 layer. In the earlier studies on the oxidation of FeCrAl alloys under gaseous environments [13–15], the major effect of S segregation was found to influence interfacial pore formation and to deteriorate the oxide scale adhesion properties. Oxides on the S-segregated region are believed to initiate cracks more easily and allow oxygen ingress. The chromium sulfides (CrS, Cr_2S_3) are thermodynamically unstable under oxygen ingress conditions. If LBE penetrates through the defects of Al_2O_3 layer and contacts with the chromium sulfides, these unstable chromium sulfides may be dissolved by LBE.

In the earlier studies on FeCrAl alloys under LBE environments [8–10], however, the S segregation was not reported. The long-term stability of Al_2O_3 layer formed on FeCrAlY coating layer homogenized by an electron pulse of GESA has been proven at 600 °C [8,9]. It is difficult to discuss the long-term stability of Al_2O_3 on the FeCrAlY coating layer with respect to S segregation effect because there is no information on the amount of S in the coating layer. However, it could be expected that the amount of S in FeCrAlY layer can be reduced during re-melting process by intense pulsed electron beams (GESA) [16]. Furthermore, the re-melting process by GESA can lead to a very fine grain microstructure on coating layer [17] which is generally effective to enhance the self-healing capability of oxide layer.

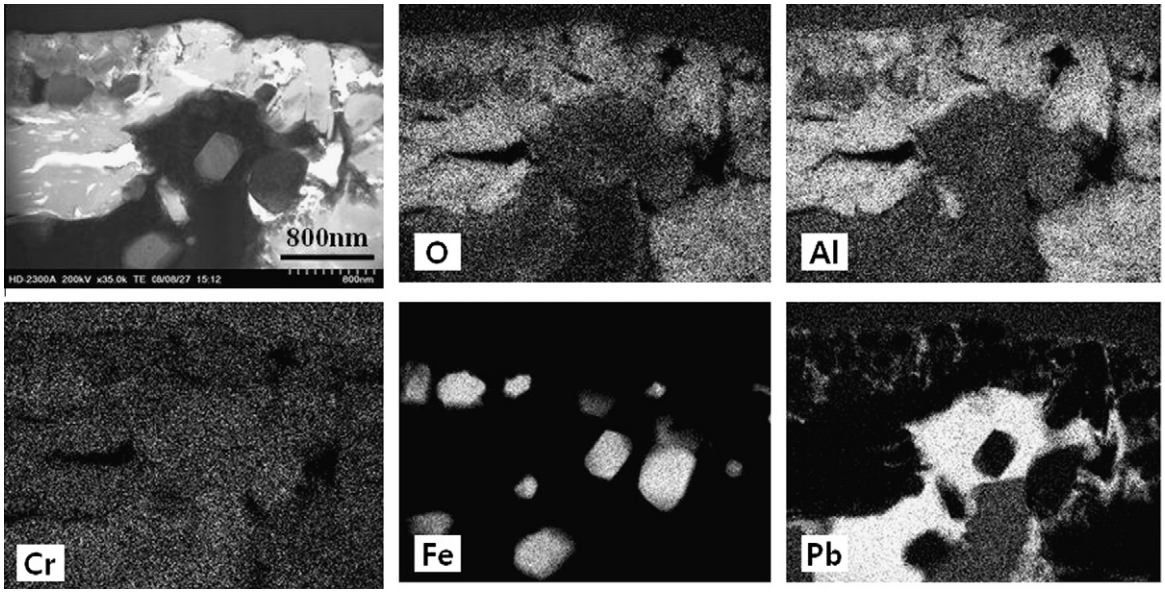

Fig. 4. STEM image and maps of cross sectional chemical composition of Kanthal-AF® after immersion in 550 °C stagnant LBE for 500 h obtained by EDS.

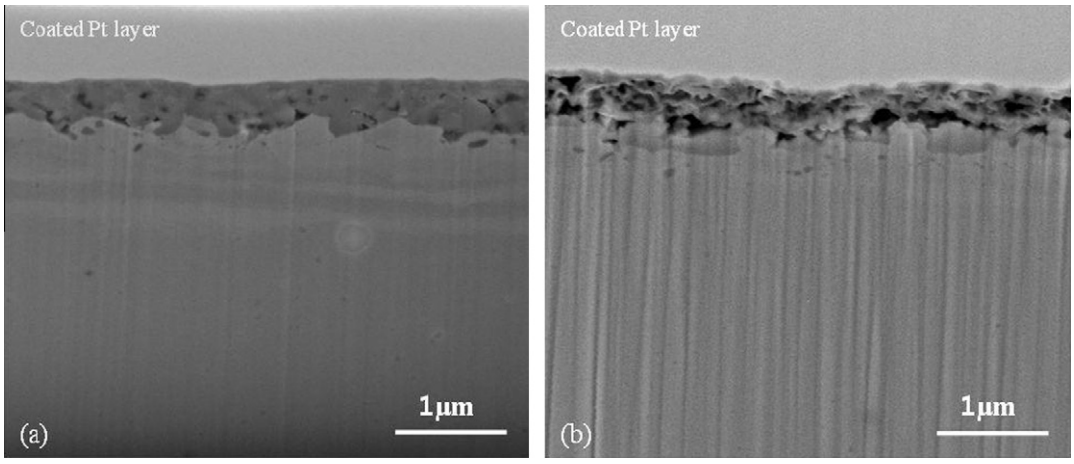

Fig. 5. FE-SEM images of the cross section of MA956 after immersion in 500 °C (a) and 550 °C (b) stagnant LBE for 500 h.

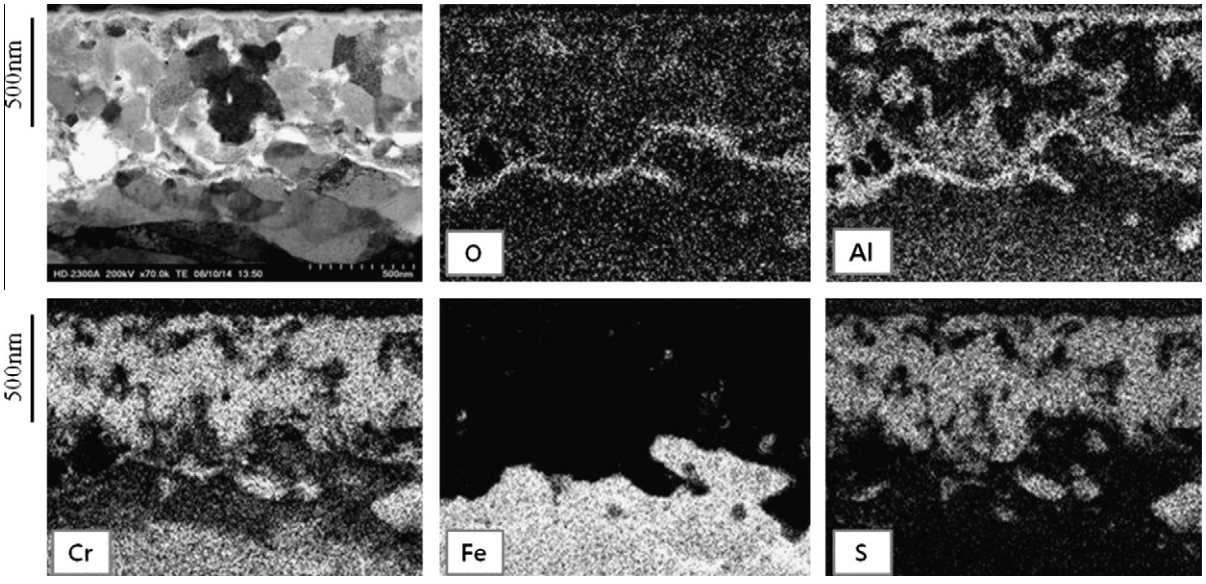

Fig. 6. STEM image and maps of cross sectional chemical composition of MA956 after immersion in 500 °C stagnant LBE for 500 h obtained by EDS.

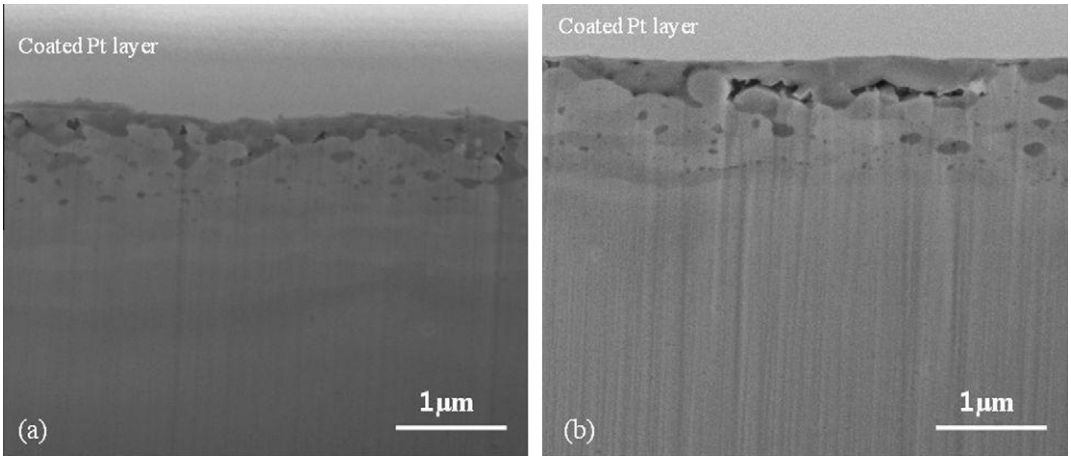

Fig. 7. FE-SEM images of the cross section of PM2000 after immersion in 500 °C (a) and 550 °C (b) stagnant LBE for 500 h.

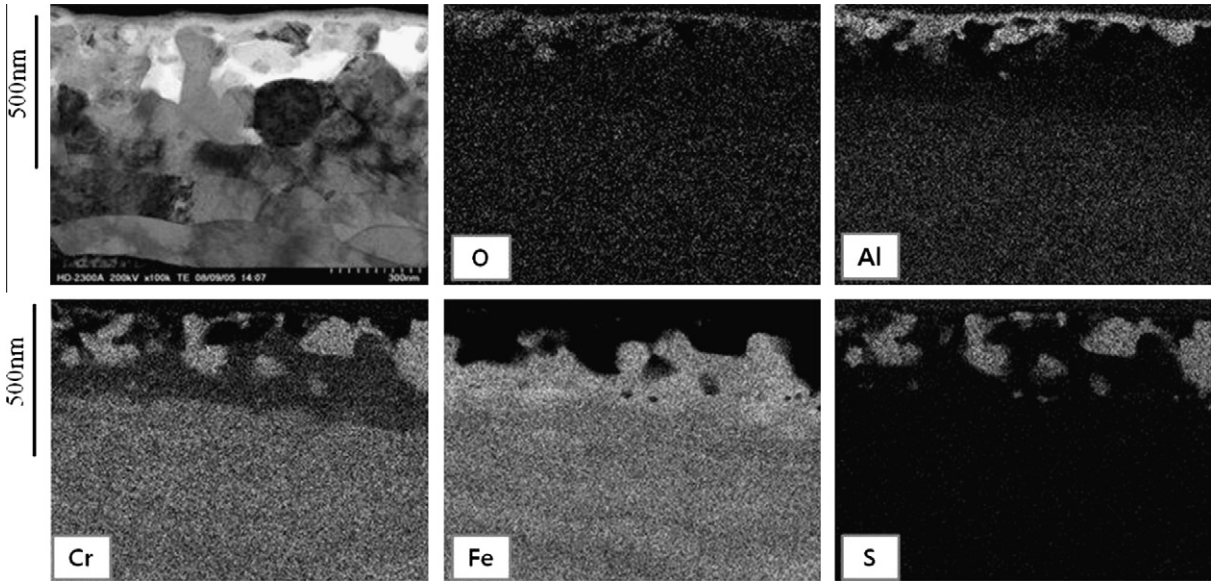

Fig. 8. STEM image and maps of cross sectional chemical composition of PM2000 after immersion in 500 °C stagnant LBE for 500 h obtained by EDS.

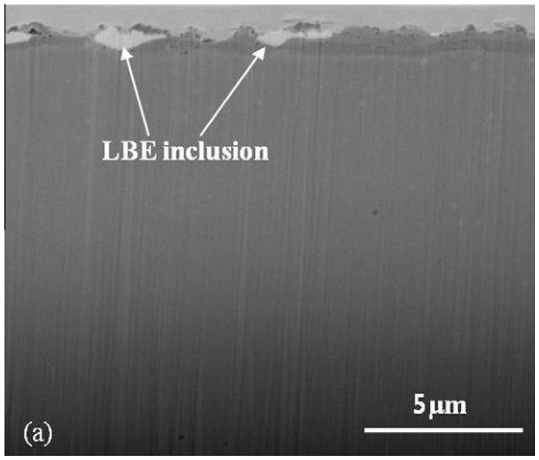

Fig. 9. FE-SEM image of the cross section in the scale-spalled region of the cross section of PM2000 after immersion in 550 °C stagnant LBE for 500 h.

Although MA956 contains higher amount of S than Kanthal-AF®, MA956 showed superior corrosion resistance by forming inner Al_2O_3 layer in this study. Therefore, the corrosion resistance of FeCrAl alloys in LBE depends on not only the amount of S impurity but also various factors such as grain size, Al contents and additive elements. Further experimental study is necessary to clarify the cause of the difference of corrosion behavior between Kanthal-AF® and MA956. Longtime corrosion tests are needed to discuss long-term stability of Al_2O_3 layer with chromium sulfides in LBE environment.

5. Conclusion

Corrosion behaviors of three types iron-based alumina forming alloys (Kanthal-AF®, MA956, PM2000) were investigated in stagnant LBE at 500 and 550 °C for 500 h. From this study, following conclusions are made:

– In 500 °C tests, thin Al_2O_3 layers were formed on the surface of all tested materials and there was no dissolution attack by LBE.

The existence of the chromium sulfide (CrS) island at the Al_2O_3 layer/metal interface was found on all tested materials. The inner Al_2O_3 layer formed on MA956 while the inner Al_2O_3 layer did not form on Kanthal-AF® and PM2000.

- At 550 °C, it is found that LBE penetrates into the metal of Kanthal-AF® through the damaged oxide layer and along the grain boundary of the metal. The penetrated depth of LBE is about 20 μm. In case of ODS materials (MA956, PM2000), the penetration of LBE into the metal was not observed.
- It was shown that FeCrAl ODS steels (PM2000, MA956) are superior resistant to corrosion compared with the FeCrAl ferritic steel (Kanthal-AF®) in LBE at higher temperature.

Acknowledgements

This work is outcome of the fostering project of the Ministry of Knowledge Economy (MKE) and financially supported by the Korean Nuclear R&D Program organized by National Research Foundation (NRF) of Korea in support of the Ministry of Education, Science and Technology (MEST). The authors are grateful to Dr. Ning Li, Peter Hosemann at LANL, Sandvik Korea Co. and Dr. Jin-Sung Jang at KEARI for providing materials.

References

[1] B.F. Gromov, Y.S. Belomitcev, E.I. Yefimov, M.P. Leonchuk, P.N. Martinov, Y.I. Orlov, D.V. Pankratov, Y.G. Pashkin, G.I. Toshinsky, V.V. Chekunov, B.A. Shmatko, V.S. Stepanov, Nucl. Eng. Des. 173 (1997) 207.
[2] N. Li, Prog. Nucl. Energy 50 (2008) 140.
[3] T.R. Allen, D.C. Crawford, Sci. Technol. Nucl. Installations 2007 (2007) 97486.
[4] I.S. Hwang, S.H. Jeong, B.G. Park, W.S. Yang, K.Y. Suh, C.H. Kim, Prog. Nucl. Energy 37 (2000) 217.
[5] I.S. Hwang et al., in: Proceedings of 2008 International Congress on Advances in Nuclear Power Plants (2008), June 8–12, 2008, Anaheim, California, USA, Paper # 8311.
[6] J. Zhang, N. Li, J. Nucl. Mater. 373 (2008) 351.
[7] D. Strauss, G. Müller, G. Schumacher, V. Engelko, W. Stamm, D. Clemens, W.J. Quaddakers, Surf. Coat. Technol. 135 (2001) 196.
[8] A. Weisenburger, A. Heinzel, G. Müller, H. Muscher, A. Rousanov, J. Nucl. Mater. 376 (2008) 274.
[9] A. Heinzel, M. Kondo, M. Takahashi, J. Nucl. Mater. 350 (2006) 264.
[10] P. Hosemann, H.T. Thau, A.L. Johnson, S.A. Maloy, N. Li, J. Nucl. Mater. 373 (2008) 246.
[11] A.K. Rivai, M. Takahashi, Prog. Nucl. Energy 50 (2008) 560.
[12] H.O. Nam, J. Lim, D.Y. Han, I.S. Hwang, J. Nucl. Mater. 376 (2008) 381.
[13] P.Y. Hou, Annu. Rev. Mater. Res. 38 (2008) 275.
[14] R. Molins, I. Rouzou, P. Hou, Mater. Sci. Eng. A 454–455 (2007) 80.
[15] P. Hou, J. Stringer, Oxid. Met. 38 (1992) 323.
[16] Y.M. Efimenko, A.B. Kuslitskii, D.V. Chaban, G.V. Karpenko, B.A. Movchan, Mater. Sci. 1 (1966) 333.
[17] R.G. Wellman, A. Scrivani, G. Rizzi, A. Weisenburger, F.H. Tenailleau, J.R. Nicholls, Surf. Coat. Technol. 202 (2007) 709.